

A Realistic Radar Simulation Framework for CARLA

Supplementary Materials

Anonymous CVPR submission

Paper ID 12354

001

1. Overview

002
003
004
005
006
007
008
009
010
011
012
013

The results from the main manuscript quote driving scores, route completion scores and infraction penalties among other scores, however they serve as an abstract representation of the actual performance of the end-to-end driving models, especially in high-risk situations. In this supplementary material, we provide a detailed route-wise analysis of all our models, highlight instances where the model undergoes infractions and provide driving videos for the same. We also provide videos of specific situations¹ wherein the ego vehicle is placed in a safety critical scenario and successfully avoids crashes due to enhanced spatial awareness from integrating Shenron radar [1].



Figure 1. Aerial view of Route 3, located in Carla Town 2. Image taken from [here](#).

014
015
016
017
018
019

We have also attached a complete driving video of Route 3 with FBLR radar view, and the overview of the route can be seen in Figure 1. Additionally, we utilize the shenron to conduct an ablation study that demonstrates the significance of angular resolutions by varying the number of antennas and analyze its impact on driving performance.

¹Due to size constraints, only the clips showing safety-critical instances from the full recordings have been included.

2. Detailed Route-wise Analysis

020
021
022
023
024
025
026
027
028
029

In the paper, we have performed evaluations on three radar views, namely Front Only, Front+Back(abbreviated as FB) and Front+Back+Left+Right (abbreviated as FBLR). We analyze how each of the model deals with four key safety traffic scenarios that occur in routes picked from the NEAT [2] paper. Additionally, we include specific cropped scenarios from the driving video to further clarify our claims. More information on the safety critical scenarios can be found here: <https://leaderboard.carla.org/scenarios/>.

2.1. Unprotected left turn at an intersection

030
031
032
033
034
035

This infraction type is demonstrated in Route 0, where the ego vehicle fails to detect vehicles coming straight while trying to take a left turn. This commonly occurs in the Front-Only radar model, while the FB and FBLR models don't exhibit this issue. This issue is demonstrated in Figure 2.

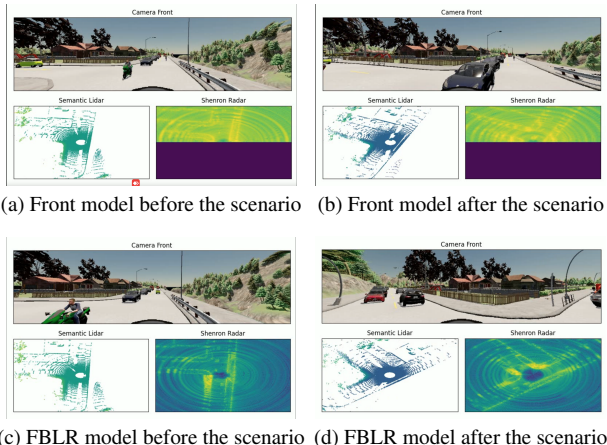


Figure 2. Comparison of driving video for Front and FBLR: (a) Before the safety scenario in Front model, (b) After the safety scenario in Front model, (c) Before the safety scenario in FBLR model, (d) After the safety scenario in FBLR model.

036

037

2.2. Crossing negotiation at a roundabout

This type of infraction is observed on Route 5 at a roundabout, where the ego vehicle fails to yield when entering the roundabout while another vehicle is approaching from the left. In some instances, a collision is narrowly avoided because the other vehicle stops, but in other cases, a crash occurs. With the Front-Only and FB radar models, collisions are observed, whereas the FBLR radar model enables the ego vehicle to accelerate and narrowly avoid a crash. This highlights the limitations of relying solely on front-facing radar data, as the ego vehicle is unable to detect vehicles approaching from the left. While the FBLR model mitigates this issue by allowing the vehicle to speed up, it still results in a near-miss. The scenario is demonstrated in Figure 3.

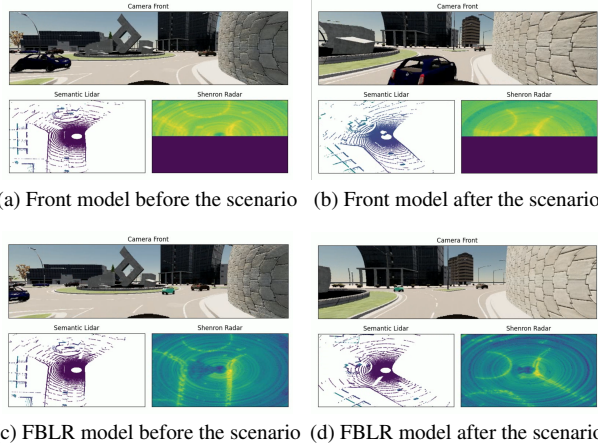


Figure 3. Comparison of driving video for Front and FBLR: (a) Before the safety scenario in Front model, (b) After the safety scenario in Front model, (c) Before the safety scenario in FBLR model, (d) After the safety scenario in FBLR model.

052

2.3. Right turn at intersection with crossing traffic

This type of infraction is observed on Route 10, where the ego vehicle fails to yield to incoming traffic from the left while attempting a right turn at an intersection. This behavior is seen in the Front-Only and FB radar models but not in the FBLR model. Depending on the timing of the traffic, the ego vehicle may avoid a collision if it begins the turn during a gap in traffic directly ahead. However, it remains at risk of a crash due to vehicles approaching from the left. Incorporating the left radar view in the FBLR model mitigates this issue by providing a wider field of view, allowing the ego vehicle to assess incoming traffic more effectively and proceed safely. This issue is demonstrated in Figure 4.

065

2.4. Vehicle invading lane on bend

This infraction type is demonstrated in Routes 1 and 3, where the ego vehicle struggles when navigating curved

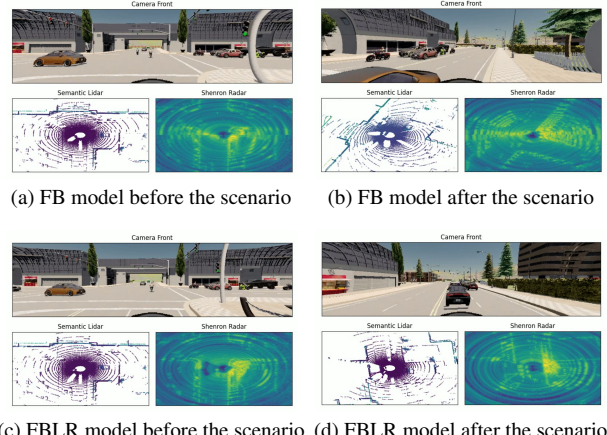


Figure 4. Comparison of driving video for FB and FBLR: (a) Before the safety scenario in FB model, (b) After the safety scenario in FB model, (c) Before the safety scenario in FBLR model, (d) After the safety scenario in FBLR model.

roads near iron railings. This infraction is exhibited in Front-Only radar model for both routes and only in route 3 for FB. This issue in route 3 is demonstrated in Figure 5.

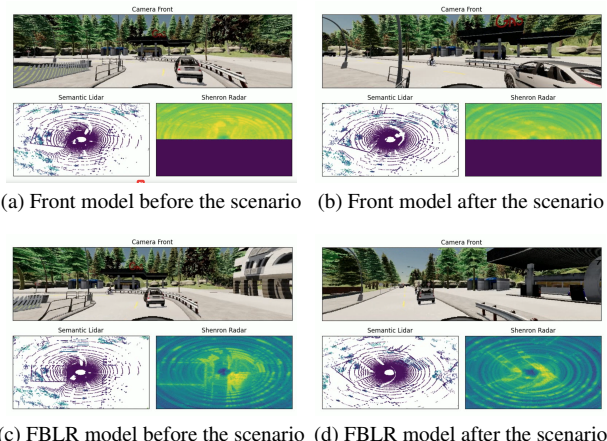
068
069

Figure 5. Comparison of driving video for Front and FBLR: (a) Before the safety scenario in Front model, (b) After the safety scenario in Front model, (c) Before the safety scenario in FBLR model, (d) After the safety scenario in FBLR model.

070
071
072
073
074
075
076
077
078

3. Resolution in Radar Sensor

The resolution of a radar sensor determines its capability to differentiate between nearby targets, which is an essential aspect affecting the radars performance in scenarios like autonomous driving, defense, and imaging systems. Radar resolution is generally divided into Range, Doppler, and Angular resolution, with angular resolution being especially crucial for modern imaging radars. In our ablations, we

079 modify the angular resolution of the radar sensor in the
 080 Shenron simulator and perform evaluations after re-training
 081 the model with this low resolution radar. We have also at-
 082 tached a full length video of Route 6 for the FBLR view.

083 3.1. Modifying the Angular Resolution

084 Angular resolution in context of radars refers to the mini-
 085 mum angular separation at which a radar system can distin-
 086 guish between two equally sized targets located at the same
 087 distance. It mainly depends on the width of the radar beam,
 088 which in-turn depends on the antenna array configuration
 089 and the wavelength of the radar signal. A key rule of thumb
 090 for angular resolution at boresight is:

$$091 \Delta\theta = \frac{2}{N}$$

092 Here, N being the number of antennas in the array. A
 093 larger number of antennas improves angular resolution by
 094 narrowing the beam-width, allowing the radar to detect
 095 finer details in its environment. For instance, Texas In-
 096 struments (TI) radar sensor [3] incorporates 86 linear an-
 097 tenna arrays, achieving high angular resolution suitable for
 098 advanced imaging applications, whereas radars like Radar-
 099 book [4], with 16 antenna arrays, provide lower angular res-
 100 olution, making them less effective for detailed analysis.

101 To highlight the importance of angular resolution, we use
 102 the Shenron simulation framework to compare the per-
 103 formance of high-resolution radar sensor (86 linear antenna
 104 array) and low-resolution radar sensor (16 linear antenna
 105 array). While the main paper focuses on evaluations using
 106 high-resolution radar sensor, this study presents evaluations
 107 using low-resolution radar sensor.

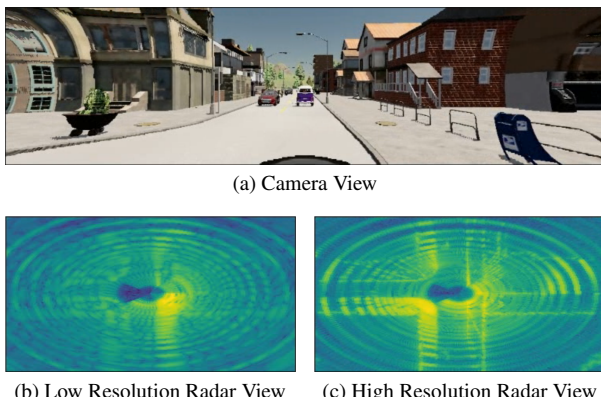


Figure 6. Comparison of radar image for a given scenario: (a) Camera View, (b) Radar view with 16 linear antenna array, (c) Radar view with 86 linear antenna array.

108 Figure 6 shows a comparison of the radar images ob-
 109 tained from the Shenron framework. Here, we generate both
 110 the low and high resolution radar view for the same scene

of the vehicle, making it very clear that latter configuration
 has a higher angular resolution than the former radar configura-
 tion.

114 3.2. Driving Results

115 As previously mentioned, we use the low resolution radar
 116 and retrain the models for Front, Front+Back, and FBLR
 117 radar views. We further evaluate the routes from the NEAT
 118 [2] paper to maintain consistency, with the FB model with
 119 86 antennas serving as the baseline for comparison, as it
 120 performed the best in terms of driving score.

Radar View	DS ↑	RC ↑	IS ↑
Front	73.82 ± 4.94	91.56 ± 2.26	0.79 ± 0.04
Front+Back	72.75 ± 6.85	92.61 ± 0.94	0.75 ± 0.07
FBLR	54.23 ± 5.84	80.69 ± 4.65	0.64 ± 0.06
Front+Back (86 Rx)	82.39 ± 4.87	97.03 ± 2.95	0.84 ± 0.03

Table 1. Results for different radar views using 16-antennas with Driving Score (DS), Route Completion (RC) and Infraction Score (IS).

121 As the results indicate from Table 1, the high-resolution
 122 FB model achieves much better results when compared to
 123 low-resolution radar configurations, mainly because of hav-
 124 ing more infractions (lower infraction score). Also we ob-
 125 serve that increasing the number of radar views paradoxically
 126 degrades performance, as evidenced by the FBLR having
 127 substantially lower driving score. This can be attributed
 128 to the blurry and imprecise nature of low-resolution radar
 129 views, which becomes problematic when multiple views are
 130 stitched together. Also a visual comparison between the two
 131 radar views from Figure 6 reveals markedly different levels
 132 of clarity and detail, explaining why simpler configurations
 133 like Front-only model outperform FBLR.

Radar View	Veh ↓	Stat ↓	Red ↓	Dev ↓	TO ↓
Front	0.58 ± 0.21	0.09 ± 0.04	0.04 ± 0.06	0.19 ± 0.08	0.14 ± 0.09
Front+Back	1.08 ± 0.26	0.03 ± 0.04	0.06 ± 0.05	0.09 ± 0.08	0.09 ± 0.09
FBLR	2.21 ± 1.13	1.70 ± 0.93	0.11 ± 0.04	1.7 ± 0.93	0.49 ± 0.11
Front+Back (86 Rx)	0.43 ± 0.12	0.01 ± 0.02	0.05 ± 0.04	0.01 ± 0.03	0.00

Table 2. Results for different radar views using 16-antennas with Vehicle Infractions (Veh), Static Object Collisions (Stat), Red Light Infractions (Red), Route Deviations (Dev) and Agent Time Outs (TO).

134 Scores from Table 2 again reinstate the point that the
 135 high resolution outperforms all other models that use low
 136 resolution radar. Also the FBLR model suffers the most in-
 137 fractions as compared to Front and FB models, which sug-
 138 gest that higher radar resolution with focused directional
 139 coverage is more effective than distributed low-resolution
 140 coverage for autonomous driving applications.

141 **4. Conclusion**

142 The FBLR radar configuration demonstrates superior per-
143 formance in most safety-critical traffic scenarios compared
144 to Front-Only and FB configurations. This is mainly be-
145 cause the FBLR configuration provides a wider field of
146 view, allowing the ego vehicle to better assess its surround-
147 ings and make safer decisions in complex traffic situations.

148 We also emphasize the crucial role of angular reso-
149 lution in radar sensor performance. The advantages of
150 high-resolution radar sensors, facilitated by larger antenna
151 arrays, demonstrates how simulation frameworks can ef-
152 fectively evaluate and optimize radar designs for specific
153 needs. These findings underscore the importance of care-
154 fully considering radar sensor configuration and resolution
155 in the development of autonomous driving systems. Note
156 that we will be releasing the radar dataset collected, code
157 and all evaluation videos upon acceptance of this paper.

158 **References**

- 159 [1] Kshitiz Bansal, Gautham Reddy, and Dinesh Bharadia. Shen-
160 ron - scalable, high fidelity and efficient radar simulation.
161 *IEEE Robotics and Automation Letters*, 9(2):1644–1651,
162 2024. 1
- 163 [2] Kashyap Chitta, Aditya Prakash, and Andreas Geiger. Neat:
164 Neural attention fields for end-to-end autonomous driving. In
165 *Proceedings of the IEEE/CVF International Conference on*
166 *Computer Vision*, pages 15793–15803, 2021. 1, 3
- 167 [3] Texas Instruments Incorporated. *Imaging Radar Using Cas-
168 caded mmWave Sensor Reference Design*. Tidep-01012 edi-
169 tion, 2019. 3
- 170 [4] INRAS. Radarbook2. 3